ISBN: 978-3-95450-227-1 ISSN: 2673-5490 doi:10.18429/JACoW-IPAC2022-MOPOPT062

FOIL FOCUSING EFFECT IN PEPPER-POT MEASUREMENTS IN INTENSE ELECTRON BEAMS*

S. Szustkowski†, M. A. Jaworski, D. C. Moir,
Los Alamos National Laboratory, Los Alamos, NM, USA

Abstract

Thin conducting foils, such as pepper-pot masks, perpendicular to an oncoming intense electron beam acts like an imperfect axisymmetric lens. The beamlets distribution from a pepper-pot mask varies based on if the mask hole radius is smaller or larger than the beams Debye length. Correcting for focusing effect is necessary for measuring transverse emittance with pepper-pot technique for intense electron beams. The Dual Axis Radiographic Hydrodynamic Test Facility (DARHT) Axis-I produces a 20 MeV, 2 kA, 80 ns FWHM electron beam for flash radiography. In this paper, we explore the effect of foil focusing due to various pepper-pot masks at DARHT Axis-I injector region from a 55 mm velvet cathode.

INTRODUCTION

Diagnostics of charged particle beams is a critical component in accelerators in understanding the underlying physics and attributes of the beam such as the emittance. One such diagnostic is pepper-pot emittance measurements, where a single shot is used to obtain data [1], whereas a solenoid scan requires several shots [2]. In the regime of intense relativistic electron beams (IREB), thin conducting foils, such as a pepper-pot mask, shorts out the transverse electric field of the beam. This causes a pinching effect to the beam due to its self-magnetic field. The transverse radial momentum receives a kick, thus the beam will have a focusing effect [3,4].

For a thermal distribution the normalized thermal beam emittance, for a given effective beam radius a, is defined as [5]

$$\epsilon_n = 2a\sqrt{\frac{k_B T\gamma}{mc^2}}, \tag{1}$$

where T is the beam transverse temperature in the laboratory frame. The beam acts like a non-neutral plasma, with density n_e, such that local charge perturbation of the beam distribution in an external focusing field will be shielded off at a distance corresponding to the Debye length λ_D. The Debye length is defined as

$$\lambda_D = \sqrt{\frac{\epsilon_0 k_B T\gamma^2}{n_e q^2}}. \tag{2}$$

When self-field effects dominate the beam, the beam radius is larger compared to the Debye length ($\lambda_D \ll a$), and the distribution is uniform. Whereas if the Debye length is larger compared to the beam radius ($\lambda_D \gg a$), the beam will be emittance dominated, exhibiting single particle behavior, and the distribution is Gaussian [6].

Using the definition of the Alfvén current limit, $I_A = 4\pi\epsilon_0 mc^3\beta\gamma/q$, and beam current, $I_B = n_e q a^2 \pi\beta c$, combining them with Eqs. (1) and (2) the Debye length can be rearranged in terms of the normalized emittance and beam current as

$$\lambda_D = \frac{\epsilon_n}{4}\sqrt{\frac{I_A}{I_B}}. \tag{3}$$

For the same initial beam attributes in varying external focusing field, the Debye length remains constant. In IREBs the Debye length is on the same order as machined holes in a pepper-pot mask. The evolution of beamlets that are produced by the mask will propagate differently based on the hole diameter.

EXPERIMENTAL ARRANGEMENT

The experiment was taken in the injection region of DARHT Axis-I, where a 55 mm velvet cathode was used. The electron beam energy during measurements was 3.25 MeV, with a current of 1.6 kA. A pepper-pot mask was placed at 41.3 cm, and 13.9 cm respectively, from an optical transition radiation (OTR) screen. The OTR screen is situated 50° to the beamline. During the run with a Debye mask it was placed 13.9 cm away from the OTR detector as illustrated in Fig. 1.

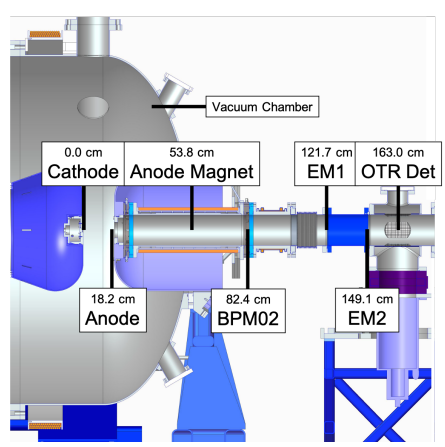

Figure 1: DARHT Axis-I injector region.

The pepper-pot mask has hole diameter of 2.0 mm with a rectangular grid spacing of 7.5 mm. The Debye mask

* Work supported by the US Department of Energy through the Los Alamos National Laboratory. Los Alamos National Laboratory is operated by Triad National Security, LLC, for the National Nuclear Security Administration of the U.S. Department of Energy (Contract No. 89233218CNA000001).
† sszustkowski@lanl.gov

ISBN: 978-3-95450-227-1 ISSN: 2673-5490 doi:10.18429/JACoW-IPAC2022-MOPOPT062

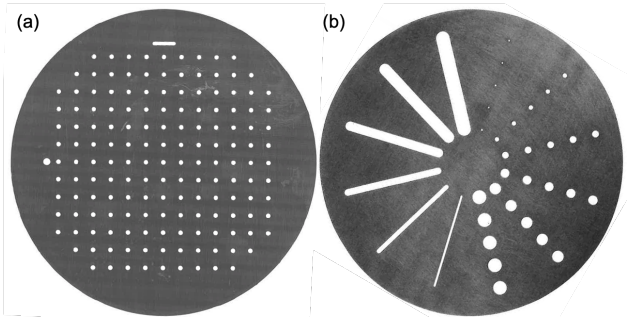

Figure 2: (a) Pepper-pot mask. (b) Debye mask with varying hole diameters.

was made with azimuthal asymetry pattern where the hole diameters range from 1-6 mm in steps of 1 mm. The radial spacing between holes is 20 mm. The rectangular slit mirrors the respective hole diameter with the same width, but each slit has a length of 80 mm. A 0.25 mm diameter reference hole was placed in the middle of the Debye mask. Figures 2a and 2b is the machined pepper-pot mask and Debye mask, respectively. A gated intensified CCD camera with a 200-500 mm, *f*/5.6, zoom lens was used to image the OTR screen. The gate width for all measurements was 10 ns at the flat top of the beam.

RESULTS

Pepper-pot mask

From previous solenoid magnet sweep scan [2], the beam emittance is determined to be 1180 π-mm-mrad. Where from the pepper-pot mask measurement the emittance is 1620 π-mm-mrad using M. Zhang formalism [1,7]. Figure 3 is a pepper-pot image from the injector with the beamlets having a Gaussian distribution. However, the analysis by Zhang's method for pepper-pot uses linear extrapolation from the imaged beam to the mask to determine the beamlet RMS divergence. Comparing the RMS divergence of the results for an on axis beamlet to the envelope code XTR [8], it is a factor of 1.5 difference. Thus, the corrected pepper-pot emittance is 1080 π-mm-mrad.

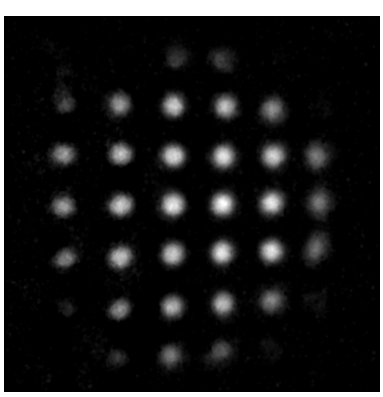

Figure 3: Pepper-pot image.

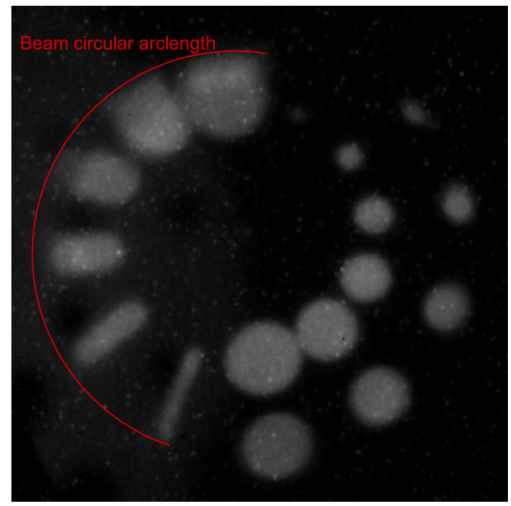

Figure 4: Debye mask image for AM = 181 A. The red line indicates the circular arc length for approximating beam radius.

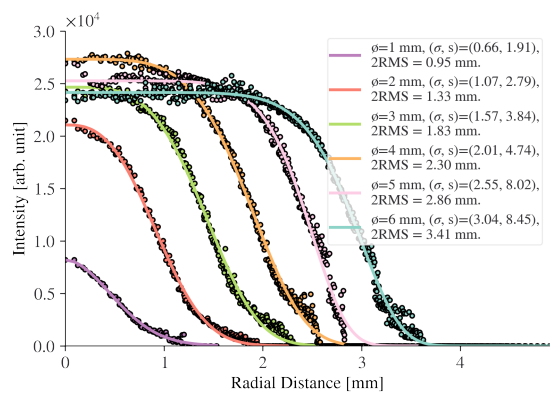

Figure 5: Radial distributions of beamlets for AM = 181 A.

Debye mask

Assuming a uniform beam and using DARHT Axis-I injector parameters, the Debye length of the beam, from Eq. (3), is 2.39 mm. For each beamlet imaged from the Debye mask, the center of mass of the intensity and the radial distribution are calculated. The radial beam profile for each beamlet is fitted to a generalized distribution and the RMS of the distribution is calculated from the fitted parameters as described in the Appendix. The overall beam size was determined by overlaying a circular arc length on the rectangular beamlet edges, which is used to validate the envelope code XTR. Figure 4 is the resulting image using the Debye mask, at anode magnet (AM) current setting of 181 A with the arc length in red. For the corresponding radial distributions and fit of the beamlets are plotted on Fig. 5.

The fitting parameter s describes the shape of the curve, such that when $s = 2$ the distribution is Gaussian, and when $s \to \infty$ the distribution is uniform. The beamlet passing through a 1 mm diameter hole the distribution is fairly Gaussian, with $s = 1.91$, however the peak intensity ~3

ISBN: 978-3-95450-227-1 ISSN: 2673-5490 doi:10.18429/JACoW-IPAC2022-MOPOPT062

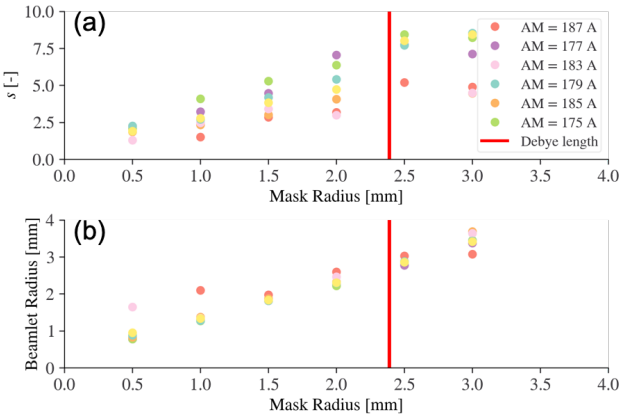

Figure 6: Fitting parameter s (a) and 2RMS (b) of beamlets through respective hole diameter for various solenoid magnet strength. The red line marks the beams Debye length.

times lower than the beamlets passing through hole diameter greater than 3 mm. As the hole diameter is increased, s increases to 8.45 for a 6 mm diameter.

For each focusing strength, the beamlet distribution is nearly Gaussian for diameters 1 and 2 mm. The distribution of the beamlets approaches to a uniform distribution with increasing hole diameter, as shown in Fig. 6a. However, these distribution disperses at varying solenoid focusing strength, since the beam radius and transverse temperature changes at the foil. The beamlet distribution from a higher beam density and smaller beam radius hitting the foil will be Gaussian-like at diameter smaller than the Debye length. The beamlets 2RMS scales linear with respect to the Debye mask hole diameter for all solenoid strengths, as shown in Fig. 6b.

CONCLUSION

The beamlet distribution was explored in an IREB using a Debye mask that consists of varying size holes. For pepper-pot measurements in IREB's, the beamlet distribution will vary based on the hole diameter, where it will be Gaussian-like at diameter's smaller than the beam's Debye length. However, using the generalized distribution fitting the RMS is consistent for varying solenoid strengths. Further work on off-axis beam and beamlets is being explored.

ACKNOWLEDGMENTS

The authors would like to thank Alex Press for fruitful discussions and the operations team at DARHT.

APPENDIX

A generalized normal distribution of random variable x, with parameters μ as the mean, σ and s as the defining features of the distribution curve, the probability density function (p.d.f.) is given by [9]

$$f(x) = \frac{s}{2\sigma\Gamma(1/s)} \exp\left\{-\left|\frac{x-\mu}{\sigma}\right|^s\right\}, \tag{4}$$

and the 2nd-order moment of the distribution is defined as

$$\mathrm{E}(x^2) = \frac{\sigma^2\Gamma(3/s)}{\Gamma(1/s)}, \tag{5}$$

where $\Gamma(n)$ denotes the Gamma function. The generalized p.d.f. includes the Gaussian distribution when $s = 2$, Laplace distribution when $s = 1$, and uniform distribution when $s \to \infty$. For varying s parameter the generalized p.d.f. is shown in Fig. 7.

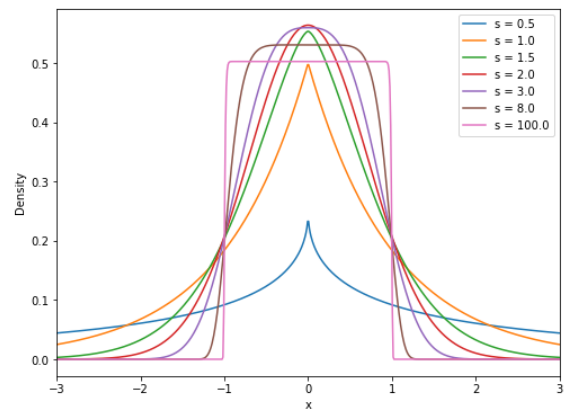

Figure 7: Generalized distribution p.d.f. for varying s values.

REFERENCES

[1] M. Zhang, "Emittance formula for slits and pepper-pot measurement", FNAL, Batavia, IL, USA, Rep. FERMILAB-TM-1988, Oct. 1996.

[2] A. F. Press, D. C. Moir, and S. Szustkowski, "Experimental Verification of DARHT Axis 1 Injector PIC Simulations", presented at the IPAC'22, Bangkok, Thailand, Jun. 2022, paper WEPOTK054, this conference.

[3] K. A. Schultz, G. T. Ortiz, M. E. Schulze, C. Carlson, and D. Guerrero, "Novel Emittance Measurement Combining Foil Focusing and Pepper-Pot Techniques", in *Proc. North American Particle Accelerator Conf. (NAPAC'19)*, Lansing, MI, USA, Sep. 2019, paper THZBB3, pp. 961–964.

[4] R. J. Adler, "Image-field focusing of intense ultra-relativistic electron beams in vacuum", *Part. Accel.*, vol. 12, pp. 39–44, 1982.

[5] M. Reiser, *Theory and Design of Charged Particle Beams*. Weinheim, Germany: Wiley-VCH, 2008.

[6] M. Reiser and N. Brown, "Thermal distribution of relativistic particle beams with space charge", *Phys. Rev. Lett.*, vol. 71, p. 2911, Nov. 1993.

[7] S. G. Anderson, J. B. Rosenzweig, G. P. LeSage, and J. K. Crane, "Space-charge effects in high brightness electron beam emittance measurements", *Phys. Rev. ST Accel. Beams*, vol. 5, p. 014201, Jan. 2002.

[8] P. W. Allison, "Beam Dynamics Equations for xtr", LANL, Los Alamos, NM, USA, Rep. LA-UR-01-6585, Dec. 2001.

[9] S. Nadarajah, "A generalized normal distribution", *Journal of Applied Statistics*, vol. 32, pp. 685-694, 2005.